https://dx.doi.org/10.4314/dujopas.v10i3a.15
ISSN (Print): 2476-8316
ISSN (Online): 2635-3490
Dutse Journal of Pure and Applied Sciences (DUJOPAS), *Vol. 10 No. 3a September 2024*

Structural Characterization and Dosimetric Response Evaluation of $(SnO)_{0.3}(TiO_2)_{0.7}$ Thin Film

Akuso C. Christopher[1*], Umaru Ibrahim[1], Yusuf S. Dauda[1], Shivil T. Jude[2], Idris M. Mustapha[3], Abdullahi A. Mundi[3]

[1]Department of Physics,
Nasarawa State University,
Keffi
Nigeria.

[2]Department of Physics,
Joseph Sarwuan Tarka University,
Makurdi
Nigeria.

[3]Nasarawa State University
Keffi,
Nigeria.

Email: akosochristopher@gmail.com

Abstract

This study investigates the effect of X-ray radiation on the I-V characteristics of $(SnO_2)_{0.3}(TiO_2)_{0.7}$ thin film in a voltage range of 0- 8 The thin film was developed using the aerosol assisted chemical deposition technique. The amorphous character of the films was shown by the XRD spectra, which showed peaks corresponding to SnO_2 and TiO_2. Smooth surface morphology with tiny poses was indicated by the FESEM picture, and 2.73 µm film thickness was identified in the cross-sectional investigation. The I-V characteristics result indicates that the electrical conductivity changes throughout a range of applied voltages, from 0 to 8 V. The I-V characteristic measurements obtained during irradiation with X-ray dosage (dose rate) ranging from 100 cGy (250 cGy/min) to 200 cGy (350 cGy/min) and a voltage range of 1.0V to 8.0 V indicate that the current increases linearly with X-ray doses and dose rate. The thin film's ability to undergo structural changes due to X-ray radiation makes it a valuable dosimetric sensor.

Keywords: Thin film, AACVD, Dosimetry, Characterization.

INTRODUCTION

The need for transparent conducting oxides (TCOs) is driven by the expansion of optoelectronic applications, including solar cells, electrochromic devices, and flat panels. (Kamrosni *et al*., 2022; Li *et al*., 2021). Non-stoichiometric and doped films of oxides of zinc, indium, cadmium, and their various alloys, produced by different methods, exhibit high reflectance in the infrared spectrum, high transmittance in the visible optical range, and extremely high conductivity (Kamrosni *et al*., 2022; Suriyani *et al*., 2023; Younus *et al*., 2021). Some of the applications for TCOs, based on these remarkable properties, include thick-film

Author for Correspondence

sensors, organic light-emitting diodes, gamma sensors, light-emitting diodes, liquid-crystalline displays, heat mirrors, dye-synthesized solar cells, wave guide electron devices, and transparent electrodes in solar cells (Bappa *et al*., 2019; Doula *et al*., 2021; Li *et al*., 2021). Typically, TCOs are produced in both undoped and doped forms from indium oxide (In_2O_3), tin oxide (SnO_2), zinc oxide (ZnO), and cadmium oxide (CdO). These oxides have high near-infrared reflectance, high electrical conductivity, and high visual transmittance, making them useful for energy conservation (Doyan *et al*., 2021; Kim *et al*., 2021; Tismanar *et al*., 2022).

The inexpensive manufacturing of tin oxide thin films and their stability in air conditions are well-known (Doyan *et al*., 2021). To improve its typical properties, tin oxide is commonly doped with indium, antimony, palladium, cobalt, and fluorine. Spray pyrolysis, sputtering, sol-gel, and chemical vapor deposition (CVD) are the most common methods used to deposit doped tin oxide thin films. Within CVD, there are several variations, including low pressure, plasma enhanced, and atmospheric pressure chemical vapor deposition (AP-CVD), which is an extremely efficient and cost-effective method (Doyan *et al*., 2021; Mohajir *et al*., 2022; Suriyani *et al*., 2023).

Titanium dioxide is an inorganic solid that is white in color. It is inexpensive, non-toxic, non-flammable, weakly soluble, and has excellent semiconducting characteristics (Doula *et al*., 2021; Zerwal *et al*., 2021). It is resistive to visible light due to its 3.2 eV band gap, which limits its capacity to absorb light to the near ultraviolet. The films have good transmittance values in the visible spectrum (Mohajir *et al*., 2022). It is frequently used in consumer and industrial items for surface treatment, for example. Scientists are quite excited about this for a number of applications, including photocatalysis, solar cells, gas sensors, anti-reflect coatings, and electrochromic devices (Kamrosni *et al*., 2022; Marcin *et al*., 2021; Shamma *et al*., 2021; Xu *et al*., 2021).

Tin oxide is resistant at high temperatures, physically robust, and chemically inert (Omran & Hussian, 2013). N-type semiconductors have low electrical resistance and great optical transparency in the visible spectrum. One example of such semiconductor is SnO_2 thin films. It serves as a window layer, a heat reflector, and a variety of gas sensors in solar cells (Doyan *et al*., 2021; Victoria, 2020). Tin oxide is a nonstoichiometric semiconductor with a large band gap (about 4 eV) and an indirect band gap (about 2.6 eV) (Abdullah et al., 2012; Carvalho et al., 2012a).

Several researchers have used various methods, including thermal evaporation, sputtering, chemical vapour deposition, sol–gel dip coating, painting, spray pyrolysis, hydrothermal process, and pyrosol deposition, as well as x-irradiation methods to create thin oxide layers Kamrosni *et al*., 2022; Parves *et al*., 2020) which may be expensive, bigger in size. In this research, TiO_2 doped SnO_2 thin film were prepared by using Erosol Assisted Chemical Vapour Deposition technique as well as x-ray irradiation which was aimed to produce more smally size dosimeters which are more affordable.

METHODOLOGY

Method

Chemical Synthesis

The SnO_2 precursor solution was prepared by adding powdered Tin (II) Chloride 2-hydrate ($Cl_2.Sn.2H_2O$) in Ethanol. Next, acetic acid was added to the solutions. The mixture was then

stirred with a magnetic stirrer for an hour until a clear solution formed. To make the TiO_2 precursor solution, titanium isopropoxyde ($Ti(OC_3H_7)4$), the TiO_2 precursor, was dissolved in isopropanol. At 60°C, the mixture was swirled for 10 minutes. The new mixture was stirred for fifteen minutes after the addition of acetic acid. The solution was obtained by adding methanol, and two hours later the final combination was blended. The generated SnO_2 and TiO_2 precursor solutions were co-doped at mole ratios of 0.3 and 0.7 weight percent, respectively. The solutions were allowed to reach chemical equilibrium at room temperature for a full day prior to initiating the deposition procedure (Halin *et al.,* 2023).

Thin Film Deposition

The $(SnO_2)0.3(TiO_2)0.7$ thin film was deposited by means of the aerosol assisted chemical vapour deposition (AACVD) technique. The procedure produces aerosols and deposits them onto a heated soda lime glass substrate using compressed air as a carrier gas. For this investigation, the precursor solution was added to the dispensing tank, and the substrate temperature was maintained at 450 ^{o}C by the heater. The computer program (Repetier host software interfaced computer software) set the settings, like spray rate and nozzle movement pattern. Throughout the procedure, the nozzle to substrate distance, the air flow rate, and the solution flow rate were measured and maintained. Once 10 milliliters of the precursor solution had been applied to the glass substrate, the spraying procedure was terminated. After removal, the substrate was let to cool to ambient temperature. To create the thick layer of interdigitated graphite electrodes that would operate as the electrical contacts on the prepared thin films, a digitally created photo-mask was employed (Zargou *et al.,* 2016).

Thin Film Characterisation

The prepared $(SnO_2)_{0.3}(TiO_2)_{0.7}$ thin films' structural and phase characterisations was carried out using X–ray diffraction (XRD) with Cu-K-α (λ = 1.54 Å) radiation. The primary divergence of the beam was suitably small for the required resolution of low glancing angle of incidence passage. XRD at grazing incidence was used to avoid the influence connected to the glass substrate. The operation of the instrument was done in a step scan mode of 0.004 and counts was collected for 1.91 s at each step (Halin *et al.,* 2023).

I-V Characteristics measurements and irradiation

An electrometer was used to record the induced during I-V characteristics determination of the thin-film structure that was subjected to different dose levels of gamma-ray radiation. I-V plot for the sample at each X-ray radiation dose value was presented, and the plots' fluctuation was calculated. The usual I-V plot for a given dose value was determined by treating the mean I-V plot for that dose value. The current versus dose charts for different voltages applied to the coplanar structure at varying doses of x-rays were obtained from the I-V plot. For each applied voltage in the range of 0-4.8 V, the current versus dose plot was used to measure the sensitivity, which is defined as the change in the current per unit change in the photon radiation dose. The least quantifiable dose which is the amount of gamma radiation needed to cause a change of 1μA in the films, was found for each applied voltage.

For the purpose of dosimetry, the fabricated thin film was irradiated to different doses of 0, 100, and 200 cGy respectively using an Electa Linear Accelerator. The irradiation area of the film was 5cm^2 and the thin film samples was mounted perpendicular to the beam. The thin films was irradiated in a sample holder of 50 nm diameter (Han *et al.,* 2009).

Sensitivity and minimum measurable dose calculation

The sensitivity of the $(SnO_2)_{0.3}(TiO_2)_{0.7}$ thin film sensor which is the change in the conductivity per unit change in the X-ray radiation dose per film surface area, was calculated using:

$$Sensitivity\ (\sigma) = \frac{I}{A\ x\ D}\ (mA.cm^{-2}Gy^{-1}) \quad (1)$$

where, I is the current induced in mA, A is the sensitive surface area in cm^2 of the film, and D is the dose absorbed in Gy. Kohli, A., Wang, C. C., & Akbar, S. A. (1999). Niobium pentoxide as a lean-range oxygen sensor. *Sensors and Actuators B: Chemical*, 56, 121-128.

The minimum measurable dose (MMD) of the $(ZnO)_{0.3}(TeO_2)_{0.7}$ thin film sensors which is the lowest measurable dose with a certain specific confidence level was calculated for each of the thin film sensor using:

$$MMD = \frac{I}{\sigma}\ (mGy) \quad (2)$$

where, σ is the sensitivity in $mA.cm^{-2}Gy^{-1}$ and I is the minimum current (1 mA), and D is the X-ray absorbed dose in Gy (Kohli *et al.*, 1999).

RESULT AND DISCUSSION

The fabricated $(SnO_2)_{0.3}(TiO_2)_{0.7}$ thin film was prepared by aerosol assisted chemical vapour deposition technique. The XRD patterns were recorded for $(SnO_2)_{0.3}(TiO_2)_{0.7}$ thin films is shown in Fig. 1. The diffraction patterns exhibit the main characteristic peaks, besides the typical peaks of the substrate for TiO_2 and SnO_2 in the thin film samples. The peaks due to pure SnO_2 thin film sample are (101), (111), (110), (202), (121) which correspond to the angles 25.21°, 29.71 °, 38.23°, 48.55°, and 62.87°, respectively. The peaks due to SnO_2 thin film has a rutile phase structure, and has been identified by comparing with JCPDS data. The peaks due to pure TiO_2 thin film are (110), (101), (111), (211), and (310) which correspond to the angles 23.96°, 31.90 °, 39.35 °, 53.69 °, and 62.63 °, respectively. The result obtained is in good agreement with the standard results according to the JCPDS data for SnO_2 and TiO_2. It is clear from the figure that the crystalline structure of the thin film prepared was amorphous at 450° substrate temperature.

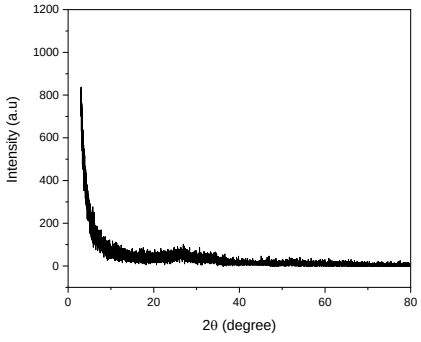

Fig. 1: XRD spectra of $(SnO_2)_{0.3}(TiO_2)_{0.7}$ thin film.

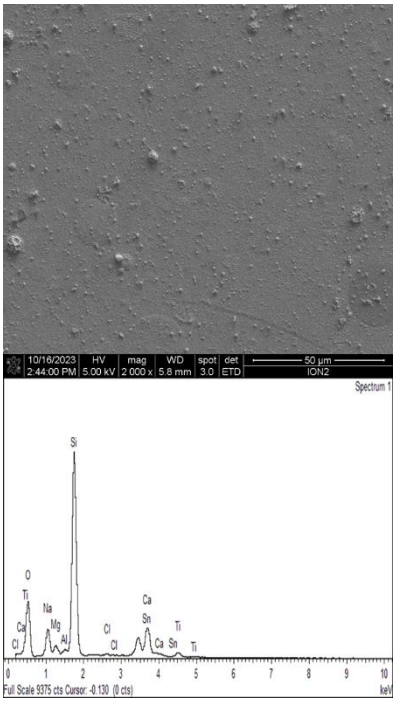

Fig. 2: FESEM image and EDX spectra of $(SnO_2)_{0.3}(TiO_2)_{0.7}$ thin film sample

It is well known that the surface morphology of the films affects their characteristics, which is crucial for applications such as X-ray and gamma sensors. It is crucial to look at the surface

morphology of the films since an increase in surface roughness causes the sensing characteristics of the films to improve.

Figure 2 displays the EDX spectra of each of the $(SnO_2)0.3(TiO_2)0.7$ thin film samples together with the corresponding FESEM image. Following a quasi-quantitative analysis of the EDX spectra, Ti, Sn, and O were found to be present in the SnO-doped TiO_2 thin film samples. These findings demonstrate that the produced films have very little magnesium contamination and a high level of purity. The comparatively high residues of soda-lime glass substrate in the EDX spectrum are not a result of the film's composition, but rather of its thinness (2.73 µm), which allows electrons to interact with the glass substrate. In addition, it was noted that, in contrast to the ideal chemical stoichiometry of SnO_2 and TiO_2, the ratios of Sn/O_2 and Ti/O_2 were less than 1.

The I-V characteristics of the synthesized $(SnO_2)_{0.3}(TiO_2)_{0.7}$ thin film was examined to demonstrate how electrical conductivity changed throughout a range of applied voltages, from 0 to 8 V. It was determined that X-ray radiation affects the I-V characteristics in order to evaluate the dosimetric response of a thin film of $(SnO_2)_{0.3}(TiO_2)_{0.7}$ as an X-ray and gamma sensor.

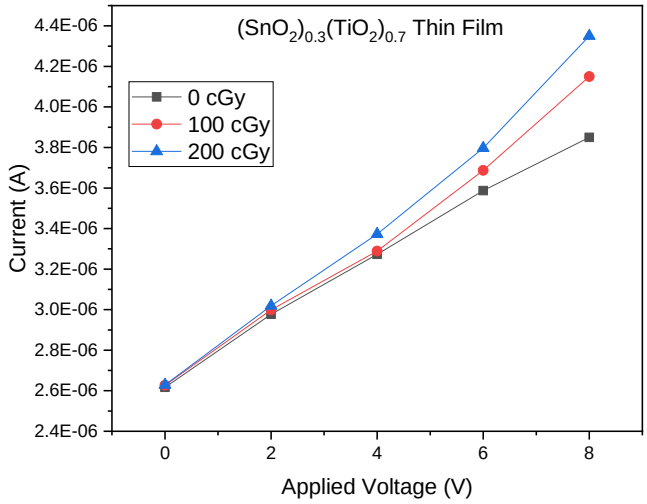

Fig. 3: Typical I-V plot at different X-ray Dose for $(SnO_2)_{0.3}(TeO_2)_{0.7}$ thin film sensor.

The measurement of I-V characteristics during irradiation was plotted for the applied voltage range of 0 - 8 V and X- ray doses of 0 cGy, 100 cGy, and 200 cGy. For all applied voltages in all thin film, the plot indicates a linear rise in the induced current as the X-ray radiation increases.

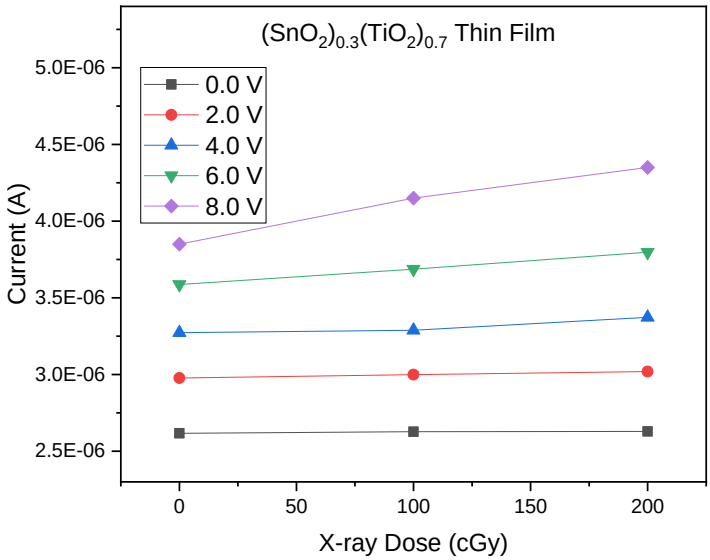

Fig. 4: Typical I-D plot at different applied Voltages for $(SnO_2)_{0.3}(TiO_2)_{0.7}$ thin film sensor.

The I-D plot during irradiation for the X- ray doses of 0 - 200 cGy and applied voltage of 0.0 - 6.0 V for each of the thin film samples. For all applied voltages in all thin film sensors, the figure indicates an increase in the induced current as the applied voltage increases.

The X-ray radiation and the film interaction causes flaws that are then transmitted through the film, causing disorder in the structure. At low doses, the thin films exhibit fine homogeneous grain structure and the number of defects (induced plus residual intrinsic defects) is lower than the number of the intrinsic defects due to the recombination of defects which increase the conductivity of the thin film, resulting in an increase in the induced current. This results correlates with those carried out by Kamrosni *et al*., (2022); Rini *et al*., (2020); Zerwal *et al*., (2021).

CONCLUSION

The purpose of the research study was to determine how X-ray radiation affects the $(SnO_2)_{0.3}(TiO_2)_{0.7}$ thin film's I-V characteristics induced current throughout a voltage range of 0 to 8 V. For each thin film sensor under investigation, the I-V characteristics generated current of the created thin film increases linearly with an increase in applied voltages. Study on the properties of I-V under X-ray exposure shows that the induced current rises linearly with X-ray dose throughout a range of 100–200 cGy for every applied voltage between 0 and 8 V. Changes created to the film microstructures during the film deposition process of the film sample could be responsible for this. This paper indicates that X-ray radiation can result in changes in microstructures, making the thin film material an invaluable dosimetric material.

REFERENCES

Abdullah, M. M., Suhail, M. H., & Abbas, S. I. (2012). Fabrication and Testing of SnO2 Thin Films as a Gas Sensor. *Journal of Thin Films*, 4(3), 1279–1288.

Bappa, S. Y., Ibrahim, U., Yusuf, S. S., Mundi, A. A., Idris, M. M., Sa'ad, H., Mohammed, A., & Soja, R. J. (2019). Performance Evaluation of Thermolumniscence Dosimeters in

Personnel in- Performance Evaluation of Thermolumniscence Dosimeters in Personnel in-Vivo Dosimetry. *Dutse Journal of Pure and Applied Sciences*, 5(March 2020), 195–203.

Carvalho, D. H. Q., Schiavon, M. A., Raposo, M. T., Paiva, R. De, Alves, J. L. A., Paniago, R. M., Speziali, N. L., Ferlauto, A. S., & Ardisson, J. D. (2012). Synthesis and characterization of SnO2 thin films prepared by dip-coating method. *Physics Procedia*, 28, 22–27. https://doi.org/10.1016/j.phpro.2012.03.664

Doula, A., Bensaha, R., & Beldjebli, O. (2021). Structural, Optical and Photocatalytic Properties of Ba-Doped TiO2 Thin Films. *Journal of ACTA Physica Polonica A*, 140(5). https://doi.org/10.12693/APhysPolA.140.421

Doyan, A., Alam, K., Muliyadi, L., Ali, F., & Awang, M. M. (2021). Synthesis and Characterization of SnO2 Thin Film Semiconductor for Electronic Device Applications. *Jurnal Penelitian Pendidikan IPA*, 7(1), 2017–2021. https://doi.org/10.29303/jppipa.v7iSpecialIssue.1270

Kamrosni, A. R., Suryani, C. H. D., Azliza, A., Mustafa, A. B. A. M., Anuar, M. S. M. A., Norsuria, M., Chobpattana, V., Kaczmarek, L., Jeż, B., & Nabiałek, M. (2022). Microstructural Studies of Ag/TiO2 Thin Film; Effect of Annealing Temperature. *Journal of Archives of Metallurgy and Materials*, 67(1), 241–245.

Kim, S., Chang, H., Kim, K. B., Kim, H., Lee, H., Park, T. J., & Park, Y. M. (2021). Highly Porous SnO2/TiO2 Heterojunction Thin-Film Photocatalyst Using Gas-Flow Thermal Evaporation and Atomic Layer Deposition. *Journal of Catalysts*, 11, 1144.

Li, C., Zhou, S., Nie, J., Huang, J., Ouyang, X., & Xu, Q. (2021). Durable Flexible Polymer-Encapsulated Cs4PbI6 Thin Film for High Sensitivity X-ray Detection. *Nano Letters*, 21(24), 10279–10283.

Marcin, Ł., Czubek, J., Drozdowska, K., Synak, A., Sadowski, W., & Ko, B. (2021). Plasmon-enhanced photoluminescence from TiO2 and TeO2 thin films doped by Eu3+ for optoelectronic applications, 1–8. https://doi.org/10.3762/bjnano.12.94

Mohajir, A. El, Arab, M., Yazdi, P., Krystianiak, A., Heintz, O., & Martin, N. (2022). Nanostructuring of SnO2 Thin Films by Associating Glancing Angle Deposition and Sputtering Pressure for Gas Sensing Applications. *Journal of Chemosensors*, 10(1), 426.

Omran, A. H., & Hussian, S. K. (2013). Structural and Optical characterization of Nanocrystalline SnO2 thin film prepared by spray pyrolysis technique. *Journal of Kufa*, 5(1).

Parves, S., Mina, S., Nahid, F., H., K. M. A., & Habib, A. (2020). Optical and Structural Properties of Vacuum Evaporated Tin Oxide (SnO2) Thin Films. *International Research Journal of Engineering and Technology*, 7(10), 1844–1849.

Rini, A. S., Deraf, M. P., & Hamzah, Y. (2020). Optical, structural and morphological studies of TiO2 thin film synthesized by liquid phase deposition method. *AIP Conference Proceedings*, 080015(May).

Shamma, K., Aldwayyan, A., Albrithen, H., & Alodhayb, N. (2021). Exploiting the properties of TiO2 thin films as a sensing layer on (MEMS)-based sensors for radiation dosimetry applications. *AIP Advances*, 025209(February), 1–9. https://doi.org/10.1063/5.0032353

Suriyani, D., Halin, C., Azliza, A., Razak, K. A., Mustafa, M., Abdullah, A., Arif, M., Mohd, A., Wahab, J. A., Chobpattana, V., Kaczmarek, L., Nabiałek, M., & Jeż, B. (2023). Characterization of SnO2/TiO2 with the Addition of Polyethylene Glycol via Sol-Gel Method for Self-Cleaning Application. *Journal of Archives of Metallurgy and Materials*, 68(1), 243–248.

Suriyani, D., Halin, C., Conf, I. O. P., Mater, S., Eng, S., Suriyani, D., Halin, C., Razak, K. A., Azani, A., & Al, M. M. (2019). Synthesis and charactherization of TiO2 doped SnO2 thin film prepared by sol-gel method. *IOP Conference Series: Materials Science and Engineering*, 701(1), 1–6. https://doi.org/10.1088/1757-899X/701/1/012003

Tismanar, I., Obreja, A. C., & Buiu, O. (2022). Composite Thin Films for Solar Photocatalytic Wastewater Treatment. *Journal of Energies*, 15.

Victoria, D. C. B. (2020). FABRICATION OF ZN DOPED SNO2 THIN FILMS AND ITS TUNING EFFECTS. *International Journal of Advanced Research in Engineering and Technology*, 11(11), 1490–1498.

Xu, S. H., Huang, J. Y., Fei, G. T., Wei, Y. S., Yuan, L. G., & Wang, B. (2021). Sol-Gel preparation of high transmittance of infrared antireflective coating for TeO2 crystals. *Journal of Infrared Physics and Technology*, 118(August), 103881. https://doi.org/10.1016/j.infrared.2021.103881

Younus, I. A., Ezzat, A. M., & Uonis, M. M. (2021). Preparation of ZnTe thin films using chemical bath deposition technique. *Journal of Nanocomposites*, 6(4), 165–172. https://doi.org/10.1080/20550324.2020.1865712

Zerwal, A. P., Khadayate, R. S., Malpure, N. N., Kasar, C. K., & Marathe, D. M. (2021). TiO2 Thin Films: A Review. *International Journal of Innovative Research in Technology*, 8(7), 563–569.

Zargou, S., Chabane Sari, S. M., Senoudi, A. R., Aida, M., Attaf, N., & Hakem, I. F. (2016). Effect of solution flow rate on growth and characterization of nanostructured ZnO thin films deposited using spray pyrolysis. *Journal of Materials and Environmental Science*, 7(9), 3134-3147.

Kohli, A., Wang, C. C., & Akbar, S. A. (1999). Niobium pentoxide as a lean-range oxygen sensor. *Sensors and Actuators B: Chemical*, 56, 121-128.

Halin, D. S. C., Azliza, A., AbdulRazak, K., Abdullah, M. M. A., MohdSalleh, M. A. A., Wahab, J. A., Chobpattana, V., Kaczmarek, L., Nabiałek, M., & Jeż, B. (2023). Characterization of SnO2/TiO2 with the Addition of Polyethylene Glycol via Sol-Gel Method for Self-Cleaning Application. *Archives of Metallurgy and Materials*, 68(1), 243-248.